

Visualization of Body Centered Cubic Energy Bands Based on Spreadsheet-Assisted Tight Binding: Solutions for Distance Material Physics Lectures

Himawan Putranta^{*}, Heru Kuswanto,
Aditya Yoga Purnama and Syella Ayunisa Rani

*Department of Educational Sciences, Concentration of Physics Education, Graduate School,
Universitas Negeri Yogyakarta, Yogyakarta 55281, Indonesia*

(*Corresponding author's e-mail: himawanputranta.2020@student.uny.ac.id)

Received: 6 October 2020, Revised: 2 July 2021, Accepted: 9 July 2021

Abstract

The development of information and communication technology also provides convenience and practicality in the world of education. In this paper, an alternative solution is presented for the discussion of energy band material in Body Centered Cubic (BCC) based on tight binding in distance material physics lectures. These activities take advantage of technology assistance in the form of spreadsheet software. Spreadsheet software is used in this research because it is a computational software that can visualize a graphic according to user commands. The use of spreadsheets is also due to being one of the computational programs that are easy to access, operate, and often used by students, especially during the current conditions affected by the Covid-19 pandemic. This research presents a simple way for students to visualize the energy band from BCC through the spreadsheet assistance. This visualization of the energy bands in BCC begins by describing the appropriate mathematical equation. Next, visualize the mathematical equation in graphical form with the spreadsheet assistance. This visualization activity can also be applied to students in material physics courses to help students understand the various characteristics of solids that have the form of BCC in everyday life. Distance material physics lectures that implement the visualization process can increase student creativity to visualize various forms of energy bands of each solid substance present.

Keywords: Body centered cubic, Distance lectures, Energy band, Spreadsheets, Visualizations

Introduction

Physics is a part of natural science that seeks to study the physical phenomena of a natural phenomenon that is so dynamic with the mathematical equation's assistance. Mathematical equations serve as a language to translate physical symptoms of a natural phenomenon that occurs in everyday life. Physics itself studies all-natural phenomena and their characteristics that occur using the mathematical equations assistance [1]. Meanwhile, material physics is a branch of physics that studies the characteristics of the material from the microscopic to the macroscopic scope that is beneficial to human life [2]. This certainly can spur material physics lecturers to further optimize the understanding and application of material physics concepts to their students in an easy, practical, varied and innovative way. In terms of optimizing the understanding and application of material physics concepts to students, a supporting medium in the form of graphic computation software is needed that can visualize abstract material physics concepts that are easily understood by students [3,4]. However, material physics lecturers also need to provide opportunities for students to visualize abstract material physics concepts into other more interesting forms, such as simulated images or videos.

Furthermore, material physics lecture activities are more optimal if students can be directly involved in the implementation of the material physics theory they have received during lectures [5]. The activities of implementing material physics theory that students have received during lectures can be done anywhere and anytime, not necessarily in the laboratory. This can also be done by utilizing existing resources such as computers to visualize material physics theory in graphical form [6,7]. Of course, these activities can be carried out distance considering the current world conditions which are experiencing the Covid-19 pandemic. Distance material physics lectures filled with activities to visualize material physics

theory in the form of graphics can improve concept understanding [8] and student creativity [9]. This is because students explore the mathematical equations of a material physics concept in detail so that they can visualize the concept in a graphic. Student creativity can grow because they can represent material physics concepts in graphical form through a variety of software. Meanwhile, one of the software that can be used anytime and anywhere to visualize physics concepts into images or graphics is a spreadsheet [10,11].

Spreadsheet software is built-in software like Microsoft Excel that is pre-installed on a computer. Of course, this spreadsheet can be used by anyone, anytime, and anywhere without an internet network to assistance visualize material physics concepts in graphical form [12,13]. Therefore, the spreadsheet software can be used to support the implementation of distance material physics courses. Instead of visualizing material physics concepts directly in the laboratory, students can visualize them on a personal computer with the spreadsheet assistance. Spreadsheets are generally graphical computing software that is easily accessible and operated by every user because they do not require complex programming languages [14,15]. Thus, spreadsheet software has been widely used to assist human activities in various sectors, one of which is the research and physics education sector.

The implementation of spreadsheets in the physics research sector can support the process of data analysis and visualization of research data in a more interactive graphical. The implementation of spreadsheets in physics education can support simple visualization constructs of each physics equation [16]. Meanwhile, the implementation of spreadsheets in physics education, especially in material physics lectures, also has a positive impact on students' abilities. This is due to spreadsheets that are easy to operate so that the integration of spreadsheets in material physics courses attracts more students to take part in these lectures [17]. Furthermore, several findings reveal the application of spreadsheet software in materials physics courses. Spreadsheet software has been used to describe electron interactions based on the tight-binding model in DNA formation [18,19]. Simulation of axial and planar ion channels in polycrystalline solids constructed using a spreadsheet [20]. The paths of charged particles in electric and magnetic fields can also be visualized using an Excel spreadsheet [21].

Although spreadsheet software has been implemented in introductory courses in material physics, the implementation of spreadsheets on advanced material physics topics such as energy bands in body centered cubic (BCC) based on the tight binding is still rare. This can occur because the translation of the mathematical equation for tight binding-based BCC energy bands is much more complex than the mathematical equations for other introductory concepts of material physics [22]. Through the visualization of mathematical equations about the BCC energy band with this spreadsheet assistance, students can be helped in describing and understanding complex equations. The implementation of spreadsheets in material physics courses also has a positive impact on students' mathematical abilities and creative thinking [23,24]. Thus, in this article, researcher present the use of graphic computing software in the form of a spreadsheet to visualize tight binding-based BCC energy bands. This visualization activity is expected to be an alternative solution for the implementation of distance material physics lectures during the Covid-19 pandemic.

Theory

The microscopic study of solids can determine the energy level of electrons and wave function in a solid or crystal system [25,26]. These studies can be useful in estimating the characteristics of each crystal in nature. One of the methods used to determine the characteristics of a crystal is by applying the Schrodinger equation solution to the interaction of electrons and ions in the crystal [27,28]. Apart from these methods, the tight-binding method is another simple method that can estimate the characteristics of crystals such as those that makeup semiconductors. The method of tight binding is generally based on the concept that a group of isolated atoms slowly fuses to form a crystal [29,30]. This method reveals that the crystal potential is interpreted as the number of identical atomic potentials and that the orbitals of each atom are identical. Therefore, the solution to the tight bond method uses a crystal wave function approximation. The crystal wave function is a linear combination of atomic orbitals and only valence electrons are referred to [31]. The crystal wave function used in this method obeys Bloch's theorem.

The study of the electron energy levels in a crystal based on the tight-binding method is carried out by considering 1 electron per atom. An electron is assumed to be in the "s" state in motion due to the influence of the crystal potential $U(r)$ of the isolated atom whose wave function is $\phi(r)$. This indicates that the influence of the other crystal atoms is small. Therefore, the crystal wave function can be written as Eq. (1) below.

$$\psi_{\vec{k}}(\vec{r}) = \sum_j C_{\vec{k}_j} \phi(\vec{r} - \vec{r}_j) \quad (1)$$

Eq. (1) shows that the sigma portion is the sum of all N lattices at the lattice point \vec{r}_j , \vec{r} is the position of the atom under consideration, and \vec{r}_j is the position of all the atoms. If the coefficient of expansion $C_{\vec{k}_j}$ is assumed to have a plane waveform, then the coefficient of expansion $C_{\vec{k}_j}$ can be written as Eq. (2) below.

$$C_{\vec{k}_j} = \frac{1}{\sqrt{N}} e^{i\vec{k} \cdot \vec{r}_j} \quad (2)$$

Eq. (1) can also be written as Eq. (3) below, but first, it with Eq. (2).

$$\psi_{\vec{k}}(\vec{r}) = \frac{1}{\sqrt{N}} \sum_j e^{(i\vec{k} \cdot \vec{r}_j)} \phi(\vec{r} - \vec{r}_j) \quad (3)$$

Eq. (3) is a form of Bloch's theorem [32]. It is assumed that the atom of a crystal moves from 1 lattice point to another ($\vec{r} \rightarrow \vec{r} + \vec{T}$), so that the equation can be shown as in Eq. (4) below.

$$\psi_{\vec{k}}(\vec{r} + \vec{T}) = e^{i\vec{k} \cdot \vec{T}} \psi_{\vec{k}}(\vec{r}) \quad (4)$$

Meanwhile, Eq. (3) can be written into other equations as shown in Eq. (5) by applying Dirac notation [33].

$$|\vec{k}\rangle = \frac{1}{\sqrt{N}} \sum_j e^{i\vec{k} \cdot \vec{r}_j} |j\rangle \quad (5)$$

where $|\vec{k}\rangle = \psi_{\vec{k}}(\vec{r})$ denotes the normalized crystal wave function and $|j\rangle = |\phi_j\rangle$ denotes the basic function of $\phi(\vec{r} - \vec{r}_j)$. The tight-binding method can also be used to find the first-order energy bands of a crystal. The step is to calculate the diagonal matrix elements using the Hamiltonian operator as shown in Eq. (6) below.

$$\langle \vec{k} | \hat{H} | \vec{k} \rangle = \frac{1}{N} \sum_j \sum_m e^{i\vec{k} \cdot (\vec{r}_j - \vec{r}_m)} (m | \hat{H} | j) \quad (6)$$

Based on Eq. (6), the element $(m | \hat{H} | j)$ can be translated into Eq. (7) below.

$$(m | \hat{H} | j) \equiv \int dV \phi(\vec{r} - \vec{r}_m) \hat{H} \phi(\vec{r} - \vec{r}_j) \quad (7)$$

Eq. (7) is the Hamiltonian volume integral equation between 2 basic functions, namely at the m and j positions [34,35]. If the elements \vec{r}_m and \vec{r}_j Eqs. (6) - (7) are replaced by the approximation $\vec{\rho}_m \equiv \vec{r}_m - \vec{r}_j$, then $\phi(\vec{r} - \vec{r}_m) = \phi(\vec{r} - \vec{\rho}_m - \vec{r}_j)$. Therefore, the energy band equation for the first order atoms of a crystal which was originally shown in Eq. (6) changes to Eq. (8) below.

$$\langle \vec{k} | \hat{H} | \vec{k} \rangle = \sum_m e^{-i\vec{k} \cdot \vec{\rho}_m} \frac{1}{N} \sum_j \int dV \phi(\vec{r} - \vec{\rho}_m - \vec{r}_j) \hat{H} \phi(\vec{r} - \vec{\rho}_j) \quad (8)$$

where $\sum_j \int dV \phi(\vec{r} - \vec{\rho}_m - \vec{r}_j) \hat{H} \phi(\vec{r} - \vec{\rho}_j) = N \int dV \phi(\vec{r} - \vec{\rho}_m) \hat{H} \phi(\vec{r})$, then the equation for the first-order energy band of a crystal atom can be written more simply as shown in Eq. (9) below. This is done by substituting equation $\sum_j \int dV \phi(\vec{r} - \vec{\rho}_m - \vec{r}_j) \hat{H} \phi(\vec{r} - \vec{\rho}_j) = N \int dV \phi(\vec{r} - \vec{\rho}_m) \hat{H} \phi(\vec{r})$ into Eq. (8).

$$\langle \vec{k} | \hat{H} | \vec{k} \rangle = \sum_m e^{-i\vec{k} \cdot \vec{\rho}_m} \frac{1}{N} \sum_j \int dV \phi(\vec{r} - \vec{\rho}_m - \vec{r}_j) \hat{H} \phi(\vec{r} - \vec{\rho}_j)$$

$$\langle \vec{k} | \hat{H} | \vec{k} \rangle = \sum_m e^{-i\vec{k} \cdot \vec{\rho}_m} \frac{1}{N} \left(N \int dV \phi(\vec{r} - \vec{\rho}_m) \hat{H} \phi(\vec{r}) \right)$$

$$\langle \vec{k} | \hat{H} | \vec{k} \rangle = \sum_m e^{-i\vec{k} \cdot \vec{\rho}_m} \left(\int dV \phi(\vec{r} - \vec{\rho}_m) \hat{H} \phi(\vec{r}) \right)$$

$$\langle \vec{k} | \hat{H} | \vec{k} \rangle = \sum_m e^{-i\vec{k} \cdot \vec{\rho}_m} \int dV \phi(\vec{r} - \vec{\rho}_m) \hat{H} \phi(\vec{r}) \quad (9)$$

If all integrals are ignored except those related to the same atom ($\vec{\rho}_{m=0} = \vec{\rho}_0$) and between the nearest neighbors (nn) the atoms associated with $\vec{\rho} \equiv \vec{\rho}_m$, then Eq. (9) can be written into Eq. (10) below.

$$\langle \vec{k} | \hat{H} | \vec{k} \rangle = e^{-i\vec{k} \cdot \vec{\rho}_0} \int dV \phi(\vec{r} - \vec{\rho}_0) \hat{H} \phi(\vec{r}) + \sum_{m=nn} e^{-i\vec{k} \cdot \vec{\rho}_m} \int dV \phi(\vec{r} - \vec{\rho}) \hat{H} \phi(\vec{r}) \quad (10)$$

Eq. (10) can be simplified again by providing several approaches to each element of its arrangement which can be shown as in Eqs. (11) - (12) below.

$$- \int dV \phi(\vec{r} - \vec{\rho}_0) \hat{H} \phi(\vec{r}) \equiv \alpha \quad (11)$$

$$- \int dV \phi(\vec{r} - \vec{\rho}) \hat{H} \phi(\vec{r}) \equiv \gamma \quad (12)$$

Furthermore, by substituting Eqs. (11) - (12) and $\vec{\rho}_0 = 0$ into equation (10), then the equation for the first-order energy band of a crystal atom can be shown as Eq. (13) below.

$$\langle \vec{k} | \hat{H} | \vec{k} \rangle = -\alpha - \gamma \sum_{m=nn} e^{-i\vec{k} \cdot \vec{\rho}_m} \equiv \varepsilon_{\vec{k}} \quad (13)$$

where $\varepsilon_{\vec{k}}$ denotes a single energy band and α is the diagonal energy associated with each electron in the crystal atom. For γ is the energy of overlap or the energy of the jump due to connecting 1 atom position to another atomic position.

Furthermore, in this article will visualize the energy bands for tight binder-based body centered cubic (BCC) crystals. Therefore, it should be noted that the crystal structure of BCC has 8 nearest neighbours associated with it which can be shown in **Figure 1** below. Materials found in everyday life that have a BCC crystal structure include lithium, sodium, potassium, chromium, barium, vanadium, alpha-iron and tungsten. Materials that have a BCC crystal structure are usually tougher than tightly packed metals such as gold [36,37].

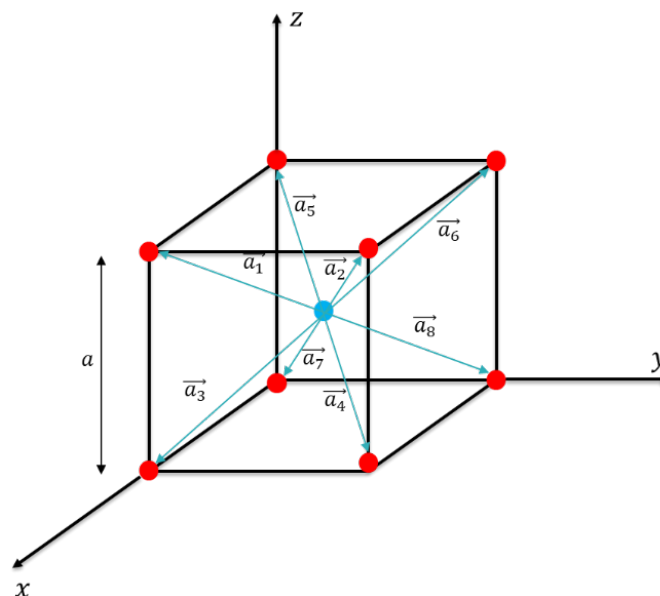


Figure 1 The 8 nearest neighbours of the BCC crystal structure.

Based on **Figure 1**, it can be shown that the blue circle shows the position of the atom being studied and the red circle shows the 8 nearest atoms. Besides, \vec{a} denotes the primitive lattice vector or the vector of displacement between atoms in terms of other atoms. In the case of BCC, 8 other atoms are the nearest neighbours of the atom under review [38]. The eight primitive lattice vectors in the BCC crystal, namely $\vec{a}_1 = \frac{1}{2}a(\hat{x} - \hat{y} + \hat{z})$, $\vec{a}_2 = \frac{1}{2}a(\hat{x} + \hat{y} + \hat{z})$, $\vec{a}_3 = \frac{1}{2}a(\hat{x} - \hat{y} - \hat{z})$, $\vec{a}_4 = \frac{1}{2}a(\hat{x} + \hat{y} - \hat{z})$, $\vec{a}_5 = \frac{1}{2}a(-\hat{x} - \hat{y} + \hat{z})$, $\vec{a}_6 = \frac{1}{2}a(-\hat{x} + \hat{y} + \hat{z})$, $\vec{a}_7 = \frac{1}{2}a(-\hat{x} - \hat{y} - \hat{z})$ and $\vec{a}_8 = \frac{1}{2}a(-\hat{x} + \hat{y} - \hat{z})$.

Based on the 8 primitive lattice vectors in the BCC crystal, there is an element a which is the distance between the nearest neighbors. The 8 primitive lattice vectors can also be written in the approximation $\vec{\rho}_m$ with the displacement rate between the atoms in question and the other atoms of 1. Therefore, the primitive lattice vector in a BCC crystal can be written as

$$\vec{\rho}_m = \frac{a}{2}[(1, -1, 1), (1, 1, 1), (1, -1, -1), (1, 1, -1), (-1, -1, 1), (-1, 1, 1), (-1, -1, -1), (-1, 1, -1)].$$

The primitive lattice vector in the BCC crystal is substituted into the element of Eq. (13), namely $\sum_{m=nn} e^{-i\vec{k}\cdot\vec{\rho}_m}$, so that the following Eq. (14) is obtained.

$$\sum_{m=nn} e^{-i\vec{k}\cdot\vec{\rho}_m} = 8\cos\left(\frac{\overline{k_x}a}{2}\right)\cos\left(\frac{\overline{k_y}a}{2}\right)\cos\left(\frac{\overline{k_z}a}{2}\right) \quad (14)$$

Eq. (14) is substituted into Eq. (13) so that the first-order energy band equation of body centered cubic (BCC) crystal atom can be shown as in Eq. (15) below.

$$\varepsilon_{\vec{k},BCC} = -\alpha - 8\gamma\cos\left(\frac{\overline{k_x}a}{2}\right)\cos\left(\frac{\overline{k_y}a}{2}\right)\cos\left(\frac{\overline{k_z}a}{2}\right) \quad (15)$$

Next, substituting Eq. (15) into the equation $E_{\vec{k}} = (\varepsilon_{\vec{k},BCC} + \alpha)/(8\gamma)$, so that the BCC crystal atomic energy band equation is obtained which can be shown as in Eq. (16) below.

$$E_{\vec{k}} = -\cos\left(\frac{\overline{k_x}a}{2}\right)\cos\left(\frac{\overline{k_y}a}{2}\right)\cos\left(\frac{\overline{k_z}a}{2}\right) \quad (16)$$

Materials and methods

In this paper, the visualization of body centered cubic (BCC) crystal atomic energy bands are performed using spreadsheet software. Spreadsheet software is used in the visualization of BCC atomic energy bands because it is easy to operate without the need for complex programming languages [39,40]. Besides, the spreadsheet also has a graphic feature with a choice of surface contours so that it can be used to plot the visualization of BCC crystal atomic energy bands based on tight banding based on Eq. (16). In this visualization, the results of the calculation of the atomic energy band of BCC crystals are plotted on the x and y axes. The element \vec{k}_x is plotted on the x -axis and \vec{k}_y on the y -axis. Furthermore, the value of a can be changed from 1 to 100 with an interval of 1 and the element $\vec{k}_z = \pi/(2a)$. The limit used for the elements \vec{k}_x and \vec{k}_y are symbolized by q whose value is between $q = +2\pi/a$ to $q = -2\pi/a$ with an interval of 0.1. Researcher e also add a spin button to the spreadsheet using developer options to change the value. This is done with the aim that the resulting BCC crystal atomic energy band visualization is more interactive. Meanwhile, the spreadsheet display used to visualize body centered cubic (BCC) energy bands based on tight binding can be shown in **Figure 2** below.

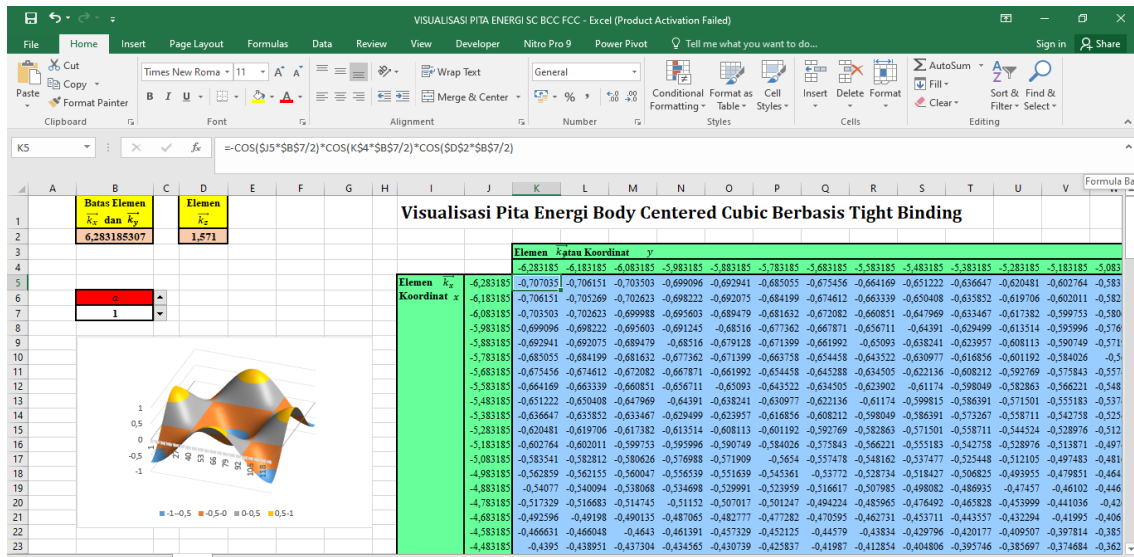


Figure 2 The spreadsheet display in the visualization of BCC energy bands based on tight binding. The list of formulas used to calculate the tight binding-based BCC energy band can be shown in **Table 1** below.

Table 1 The formula used in the spreadsheet for calculating the BCC energy band.

| Variable | Cell | Formula |
|--|----------|--|
| Element boundaries \vec{k}_x and \vec{k}_y (q) | B2 | $=2*PI()/\$B\7 |
| The nearest neighbor distance (a) | B7 | Input data between (1:100) with intervals of 1 |
| Element \vec{k}_z | D2 | $=PI()/(2*\$B\$7)$ |
| Element \vec{k}_x on the x -axis | J5-J131 | Input data between $(-q; q)$ with intervals of 0.1 |
| Element \vec{k}_y on the y -axis | K4-EG4 | Input data between $(-q; q)$ with intervals of 0.1 |
| BCC energy band | K5-EG131 | $=-COS(\$J5*\$B\$7/2)*COS(K\$4*\$B\$7/2)*COS(\$D\$2*\$B\$7/2)$ |

Results and discussion

Visualization of body centered cubic energy bands

In this article, a simple tight binding-based body centered cubic (BCC) energy band visualization is shown using a spreadsheet for various distances between the nearest neighbours (a). The visualization of the energy band distribution in the BCC crystal for the nearest neighbour distance ($a = 1, 2, 3, 4, 5$) can be shown in **Figure 3** below.

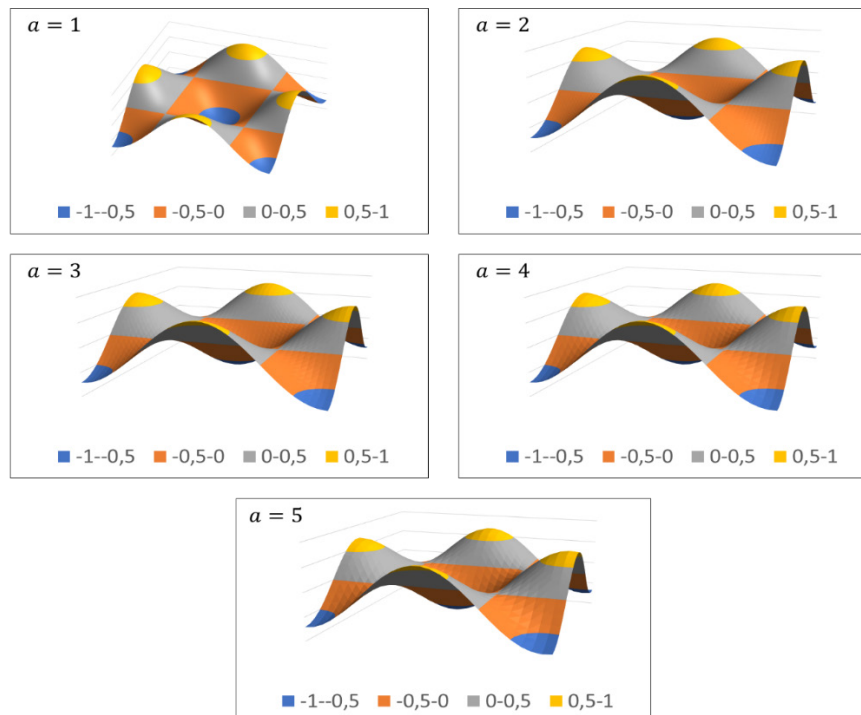


Figure 3 Distribution of energy bands in BCC crystals with $a = 1, 2, 3, 4, 5$.

Figure 3 shows the energy band distribution in the body centered cubic (BCC) crystal for $a = 1, 2, 3, 4, 5$. Visualization of the energy band distribution for $a = 1$ shows that the largest energy is in the edge, while the smallest energy is in the middle. Its energy band distribution consists of 4 half-full lobes. Meanwhile, for $a = 2, 3, 4, 5$, the visualization of the energy band distribution is the same as for the visualization of the energy band distribution for $a = 1$. The similarity in visualizing the distribution of energy bands from the five variations of the distance between the nearest atoms in the BCC crystal can be seen from the largest and smallest energy band intervals, which are in the intervals of 0.5 to 1 and -1 to -0.5 , respectively. This shows that increasing the distance between the nearest atoms in the BCC crystal will not affect the energy band distribution. However, specifically the visualization of the energy band distribution for $a = 1, 2, 3, 4, 5$ has a difference. The difference that arises from the visualization of the energy band distribution for the 5 variations of the distance between the nearest atoms in the BCC crystal is that the farther the distance between the nearest atoms or the greater the value of a or ($a > 1$), the visualization of the distribution of the energy band formed becomes stiffer or rough. The rough distribution of energy bands can be visualized on a spreadsheet with the appearance of a rhombic texture.

Based on **Figure 3**, the order of visualization of the distribution of energy bands that is the heaviest to the most rigid or coarse is the visualization of the distribution of energy bands for $a = 1$ is more subtle than the visualization of the energy band distribution for $a = 2$. The visualization of the energy band distribution for $a = 2$ is smoother than the visualization of the energy band distribution for $a = 3$. The visualization of the energy band distribution for $a = 3$ is smoother than the visualization of the energy band distribution for $a = 4$. Meanwhile, the visualization of the energy band distribution for $a = 3$ is smoother than the visualization of the energy band distribution for $a = 5$. Based on **Figure 3**, the softest energy band distribution is the energy band distribution in the BCC crystal for $a = 1$. Meanwhile, the distribution of the energy band that is the most rigid or coarse is the distribution of the energy band in the BCC crystal for $a = 5$. This is due to variations in the tenth data on the distance between the nearest atoms in the spreadsheet software that affect the components in the calculation of the BCC digital energy band based on the tight-binding method. The components in the calculation of this energy band that is affected by changes in the value of a are the minimum and maximum limit values on the x and y axes, the values on the z -axis, and the resulting energy band distribution. If the a value entered in the spreadsheet software gets bigger, the minimum and maximum limit values on the x and y axes, the values on the x and z -axis, and the number of energy bands produced will be smaller. Meanwhile, for $a > 5$, the distribution of the energy bands visualized on the spreadsheet is getting rough or stiff. This is because the

element boundaries \vec{k}_x and \vec{k}_y are getting smaller and the element value \vec{k}_z is also getting smaller. This phenomenon can be shown in **Figure 4** below.

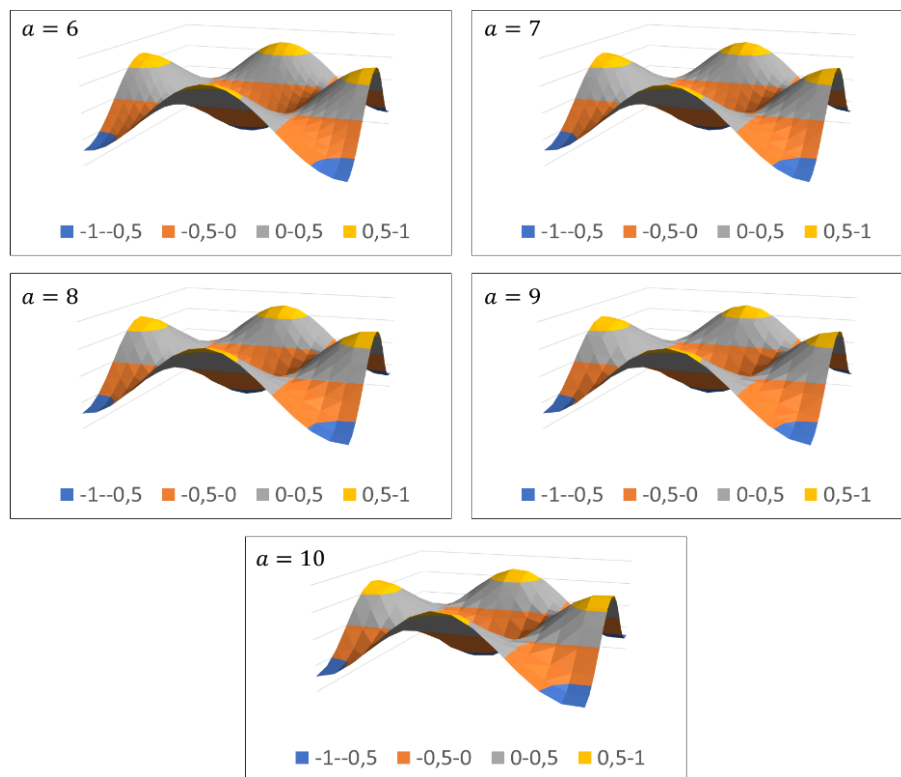


Figure 4 Distribution of energy bands on BCC crystals with $a = 6, 7, 8, 9, 10$.

Figure 4 illustrates the distribution of the energy bands in the BCC crystal with a large a . Based on **Figure 4**, it appears that the visualization of the energy band distribution in BCC crystals is getting stiffer or coarser and the energy is getting bigger. The greater the energy can be indicated by many coarse energy band distributions. Eq. (16) explains that the energy band size of the BCC crystal atoms is proportional to the distance between the nearest neighbour atoms (a). When the distance between the nearest neighbour atoms (a) gets bigger, the visualization of the energy band distribution will also be coarser or stiffer. However, when the distance between the nearest neighbours' atoms (a) gets smaller, the visualization of the energy band gets smoother. Besides, the visualization of the energy band distribution of the BCC crystals carried out in this study is consistent with the results of the visualization of previous studies. The visualization of the energy band distribution in BCC crystals with $a = 1$ shown in **Figure 3** is like the results of experiments conducted by previous researchers [41].

Implementation in distance material physics lectures

The global conditions that are currently affected by the Covid-19 pandemic have made face-to-face lectures and practicum activities difficult to do. Therefore, various online lecture innovations are mostly carried out by lecturers and students. One form of online lecture innovation, especially in the field of material physics, is to visualize mathematical equations of a physical phenomenon using the spreadsheet software assistance. As in this paper, which visualizes the atomic energy band of the body centered cubic crystal (BCC) based on the tight-binding method with the spreadsheet assistance. Through this visualization activity, students can develop analytical skills, mathematical abilities, creative thinking, and conceptual understanding of the BCC crystal energy band material based on the tight-binding method [42,43].

In the material physics lecture process that implements the use of spreadsheet software, lecturers can start by presenting material about the atomic crystal energy band based on the tight-binding method to students. Meanwhile, students are asked to understand the material physics theories presented by the

lecturer. After that, lecturers can ask their students to analyse and describe mathematical equations about the energy bands of the digital atom, especially body centered cubic (BCC) based on the tight-binding method. After students get the details of the mathematical equation from the atomic energy band of the BCC digital atom, they need to present the details of the mathematical equation. This was done to check the mathematical equation of the atomic energy bands of the BCC crystals that had been compiled by the students. Furthermore, the lecturer can divide the students into several groups to visualize the mathematical equations of the BCC crystal atomic energy bands that they have compiled using the spreadsheet assistance. The results of the energy band visualization that have been carried out by students are then presented and compared with the results of the visualization conducted by the lecturer.

This visualization activity can be a link between mathematical modelling and material physics experiments easily, can be done anytime, anywhere. This visualization activity is also can make it easier for students to apply the mathematical equations of a physical phenomenon that they get during lectures [44,45]. Thus, the activity of visualizing mathematical equations of physical phenomena can support the implementation of distance material physics courses. The implementation of material physics lectures that implements this visualization activity can be carried out well if students can be actively involved in understanding mathematical equations of physical phenomena and virtual experiments through the spreadsheet's assistance.

Conclusions

In this research, it is shown a computational software in the form of a spreadsheet that is used to visualize material physics theory. The spreadsheet software is used to visualize the atomic energy bands of body centered cubic crystals (BCC) based on the tight-binding method. The spreadsheet software was chosen to visualize the atomic energy band of BCC crystals because it is one of the computational software that is easy to operate and does not require a programming language that is too complicated, making it easy to use by students or novice programmers. This visualization activity can make it easier for students to understand and implement mathematical equations of a physical phenomenon that occurs in everyday life. The visualization activity of BCC digital atomic energy bands based on the tight-binding method can support the implementation of long-distance material physics lectures. Furthermore, the results of this research can also be used as a reference source for researchers or students in the future to be able to visualize energy bands of crystal atoms and mathematical equations of other physics phenomena.

Acknowledgements

The author would like to thank the Department of Educational Sciences, Concentration of Physics Education, Graduate School, Universitas Negeri Yogyakarta, Indonesia for supporting this research.

References

- [1] A Atangana and JF Gómez-Aguilar. Decolonisation of fractional calculus rules: Breaking commutativity and associativity to capture more natural phenomena. *Eur. Phys. J. Plus* 2018; **133**, 166-75.
- [2] SR Wilson and MI Mendeleev. A unified relation for the solid-liquid interface free energy of pure FCC, BCC, and HCP metals. *J. Chem. Phys.* 2016; **144**, 144707.
- [3] E Pratidhina, WSB Dwandaru and H Kuswanto. Exploring Fraunhofer diffraction through tracker and spreadsheet: An alternative lab activity for distance learning. *Revista Mexicana de Física* 2020; **17**, 285-90.
- [4] M Farrokhnia, HJ Pijeira-Díaz, O Noroozi and J Hatami. Computer-supported collaborative concept mapping: The effects of different instructional designs on conceptual understanding and knowledge co-construction. *Comput. Educ.* 2019; **142**, 103640.
- [5] B Gregorcic, E Etkina and G Planinsic. A new way of using the interactive whiteboard in a high school physics classroom: A case study. *Res. Sci. Educ.* 2018; **48**, 465-89.
- [6] Y Daineko, V Dmitriyev and M Ipalakova. Using virtual laboratories in teaching natural sciences: An example of physics courses in university. *Comput. Appl. Eng. Educ.* 2017; **25**, 39-47.
- [7] M Nasir, RB Prastowo and R Riwayani. Design and development of physics learning media of three-dimensional animation using Blender applications on atomic core material. *J. Educ. Sci.* 2018; **2**, 23-32.
- [8] G Gunawan, N Nisrina, NMY Suranti, L Herayanti and R Rahmatiah. Virtual laboratory to improve students' conceptual understanding in physics learning. *J. Phys. Conf. Ser.* 2018; **1108**, 012049.

- [9] G Gunawan, A Harjono, H Sahidu and L Herayanti. Virtual laboratory of electricity concept to improve prospective physics teacher's creativity. *Indonesian J. Phys. Educ.* 2017; **13**, 102-11.
- [10] PS Tambade. Trajectory of charged particle in combined electric and magnetic fields using interactive spreadsheets. *Eur. J. Phys. Educ.* 2011; **2**, 49-59.
- [11] I Nachtigalova, J Finkeova, Z Krbcova and H Souskova. A spreadsheet-based tool for education of chemical process simulation and control fundamentals. *Comput. Appl. Eng. Educ.* 2020; **28**, 923-37.
- [12] AA Gorni. *Spreadsheet applications in materials science*. In: G Filby (Ed.). *Spreadsheets in science and engineering*. Springer Berlin, Heidelberg, Germany, 1998, p. 229-60.
- [13] X Peng, N Mathew, IJ Beyerlein, K Dayal and A Hunter. A 3D phase field dislocation dynamics model for body-centered cubic crystals. *Comput. Mater. Sci.* 2020; **171**, 109217.
- [14] CJ Weiss. Scientific computing for chemists: An undergraduate course in simulations, data processing, and visualization. *J. Chem. Educ.* 2017; **94**, 592-7.
- [15] CL Lai and GJ Hwang. A spreadsheet based visualized Mindtool for improving students' learning performance in identifying relationships between numerical variables. *Interact. Learn. Environ.* 2015; **23**, 230-49.
- [16] RG Rinaldi and A Fauzi. A complete damped harmonic oscillator using an Arduino and an Excel spreadsheet. *Phys. Educ.* 2019; **55**, 015024.
- [17] I Singh and B Kaur. Teaching graphical simulations of Fourier series expansion of some periodic waves using spreadsheets. *Phys. Educ.* 2018; **53**, 035031.
- [18] H Yamada and K Iguchi. Some effective tight-binding models for electrons in DNA conduction: A review. *Adv. Condens. Matter Phys.* 2010; **2010**, 380710.
- [19] S Varela, V Mujica and E Medina. Effective spin-orbit couplings in an analytical tight-binding model of DNA: Spin filtering and chiral spin transport. *Phys. Rev. B* 2016; **93**, 155436.
- [20] EI Preiß, H Lyu, JP Liebig, G Richter, F Gannott, PA Gruber and B Merle. Microstructural dependence of the fracture toughness of thin metallic films: A bulge test and atomistic simulation study on single-crystalline and polycrystalline silver films. *J. Mater. Res.* 2019; **34**, 3483-94.
- [21] I Singh, KK Khun and B Kaur. Visualizing the trajectory of a charged particle in electric and magnetic fields using an Excel spreadsheet. *Phys. Educ.* 2018; **54**, 015002.
- [22] CC Lee, YT Lee, M Fukuda and T Ozaki. Tight-binding calculations of optical matrix elements for conductivity using nonorthogonal atomic orbitals: Anomalous Hall conductivity in bcc Fe. *Phys. Rev. B* 2018; **98**, 115115.
- [23] A Fauzi, DT Rahardjo, U Romadhon and KR Kawuri. Using spreadsheet modeling in basic physics laboratory practice for physics education curriculum. *Int. J. Sci. Appl. Sci. Conf. Ser.* 2017; **2**, 8-15.
- [24] A Singkun. Factors associated with Corona Virus 2019 (Covid-19) prevention behaviors among health sciences students of a higher education institution in Yala Province, Thailand: Covid-19 prevention behaviors. *Walailak J. Sci. Tech.* 2020; **18**, 967-78.
- [25] F Raouafi, B Chamekh, J Even and JM Jancu. Electronic and optical properties in the tight-binding method. *Chin. J. Phys.* 2014; **52**, 1376-86.
- [26] M Hohenleutner, F Langer, O Schubert, M Knorr, U Huttner, SW Koch and R Huber. Real-time observation of interfering crystal electrons in high-harmonic generation. *Nature* 2015; **523**, 572-5.
- [27] C Kittel. *Introduction to solid state physics*. 8th ed. John Wiley & Sons, New Jersey, United States, 2005.
- [28] A Jain, Y Shin and KA Persson. Computational predictions of energy materials using density functional theory. *Nat. Rev. Mater.* 2016; **1**, 15004.
- [29] JE Castellanos-Aguila, P Palacios, P Wahnón and J Arriaga. Tight-binding electronic band structure and surface states of Cu-chalcopyrite semiconductors. *J. Phys. Comm.* 2018; **2**, 035021.
- [30] SJ Caldwell, IC Haydon, N Piperidou, PS Huang, MJ Bick, HS Sjöström and C Zeymer. Tight and specific lanthanide binding in a de novo TIM barrel with a large internal cavity designed by symmetric domain fusion. *Proc. Nat. Acad. Sci.* 2020; **117**, 30362-9.
- [31] JE Hasbun and T Datta. *Introductory solid-state physics with MATLAB applications*. CRC Press, Boca Raton, Florida, United States, 2019.
- [32] H Bross. Electronic structure of the cubic compounds ReGa₃ (Re = Er, Tm, Yb, and Lu). *Adv. Condens. Matter Phys.* 2011; **2011**, 867074.
- [33] B Partoens and FM Peeters. Normal and Dirac fermions in graphene multilayers: Tight-binding description of the electronic structure. *Phys. Rev. B* 2007; **75**, 193402.
- [34] AP Sutton, MW Finnis, DG Pettifor and Y Ohta. The tight-binding bond model. *J. Phys. C Solid State Phys.* 1998; **21**, 35-47.

- [35] Y Wu and PA Childs. Conductance of graphene nanoribbon junctions and the tight binding model. *Nanoscale Res. Lett.* 2011; **6**, 62-8.
- [36] SI Rao, C Woodward, B Akdim and ON Senkov. A model for interstitial solid solution strengthening of body centered cubic metals. *Materialia* 2020; **9**, 100611.
- [37] MP Groover. *Fundamentals of modern manufacturing: Materials, processes, and systems*. John Wiley & Sons, New Jersey, United States, 2020.
- [38] H Hardhienata, TI Sumaryada, B Pesendorfer and A Alejo-Molina. Bond model of second-and third-harmonic generation in body-and face-centered crystal structures. *Adv. Mater. Sci. Eng.* 2018; **2018**, 7153247.
- [39] M Iqbal, F Ahmed, A Iqbal and Z Uddin. Teaching physics online through spreadsheets in a pandemic situation. *Phys. Educ.* 2020; **55**, 063006.
- [40] KSP Chang and BA Myers. Gneiss: Spreadsheet programming using structured web service data. *J. Vis. Lang. Comput.* 2017; **39**, 41-50.
- [41] SA Sinex and JB Halpern. Discovery learning tools in materials science: Concept visualization with dynamic and interactive spreadsheets. *Mater. Res. Soc. Symp. Proc.* 2009; **1233**, PP03-04.
- [42] T Lowrie, T Logan, D Harris and M Hegarty. The impact of an intervention program on students' spatial reasoning: Student engagement through mathematics-enhanced learning activities. *Cognit. Res. Princ. Implic.* 2018; **3**, 50.
- [43] S Jelatu. Effect of geogebra-aided react strategy on understanding of geometry concepts. *Int. J. Instruc.* 2018; **11**, 325-36.
- [44] V Mešić, E Hajder, K Neumann and N Erceg. Comparing different approaches to visualizing light waves: An experimental study on teaching wave optics. *Phys. Rev. Phys. Educ. Res.* 2016; **12**, 010135.
- [45] A Srinath. Active learning strategies: An illustrative approach to bring out better learning outcomes from science, technology, engineering, and mathematics (STEM) students. *Int. J. Emer. Tech. Learn.* 2015; **9**, 21-5.